LAWRENCE
LIVERMORE
NATIONAL
LABORATORY

UCRL-JRNL-200162

Role of Fanconi Anemia FANCG in Preventing Double-Strand Breakage and Chromosomal Rearrangement during DNA Replication

Robert S. Tebbs, John M. Hinz, N. Alice Yamada, James B. Wilson, Nigel J. Jones, Edmund P. Salazar, Cynthia B. Thomas, Irene M. Jones, Larry H. Thompson

October 7, 2003

Molecular Cell

Role of Fanconi Anemia *FANCG* in Preventing Double-Strand Breakage and Chromosomal Rearrangement during DNA Replication

Robert S. Tebbs, John M. Hinz, N. Alice Yamada, James B. Wilson[*], Nigel J. Jones[*],

Edmund P. Salazar, Cynthia B. Thomas, Irene M. Jones, and Larry H. Thompson[†]

Biology and Biotechnology Research Program, L441
Lawrence Livermore National Laboratory, P.O. Box 808
Livermore, CA 94551-0808

[*] School of Biological Sciences, Biosciences Building, Crown Street,
The University of Liverpool, Liverpool, L69 7ZB, UK

Running title: Role of *FANCG* in Preventing DNA Breakage

Key Words: FANCG, Fanconi anemia, gene targeting, mutagen survival, oxidative damage, chromosomal instability, cell cycle

Abbreviations: CHO, Chinese hamster ovary; FA, Fanconi anemia; HR, homologous recombination; ROS, reactive oxygen species; MMC, mitomycin C; MMS, methyl methanesulfonate; MNU methylnitrosourea; S^6G, 6-thioguanine

[†]To whom correspondence should be addressed (e-mail: thompson14@llnl.gov)

Summary

The Fanconi anemia (FA) proteins overlap with those of homologous recombination through FANCD1/BRCA2, but the biochemical functions of other FA proteins are unknown. By constructing and characterizing a null *fancg* mutant of hamster CHO cells, we present several new insights for FA. The *fancg* cells show a broad sensitivity to genotoxic agents, not supporting the conventional concept of sensitivity to only DNA crosslinking agents. The *aprt* mutation rate is normal, but *hprt* mutations are reduced, which we ascribe to the lethality of large deletions. *CAD* and *dhfr* gene amplification rates are increased, implying excess chromosomal breakage during DNA replication, and suggesting amplification as a contributing factor to cancer-proneness in FA patients. In S-phase cells, both spontaneous and mutagen-induced Rad51 nuclear foci are elevated. These results support a model in which FancG protein helps to prevent collapse of replication forks by allowing translesion synthesis or lesion bypass through homologous recombination.

Introduction

Fanconi anemia (FA) is a rare autosomal recessive disorder characterized by progressive bone marrow failure and cancer susceptibility, especially for acute myelogenous leukemia (Tischkowitz and Hodgson, 2003). FA is genetically heterogeneous, consisting of at least eight complementation groups for which genes have been identified: *FANCA*, *C*, *D1*, *D2*, *E*, *F*, *G*, and *FANCL/PHF9* (D'Andrea and Grompe, 2003; Meetei et al., 2003a). The role of the FA protein "pathway" in recovery of cells from DNA damaging agents is under intense investigation. FA proteins interact to form a nuclear A/C/E/F/G/L complex (Garcia-Higuera et al., 1999; Waisfisz et al., 1999; de Winter et al., 2000; Siddique et al., 2001; Pace et al., 2002; Meetei et al., 2003a; Meetei et al., 2003b). The integrity of this complex is essential for the mono-ubiquitinylation of FANCD2 following mitomycin C (MMC) or ionizing radiation (IR) treatment. Interestingly, FANCD1, D2, and L are the only FA proteins evolutionarily conserved in nonvertebrates (Timmers et al., 2001; Lo et al., 2003; Meetei et al., 2003a).

Recently, the *FANCD1* gene was found to be identical with *BRCA2* (Howlett et al., 2002), a participant in the formation of Rad51 nucleoprotein filaments during homologous recombination (HR) (Davies et al., 2001). FA-D1 mutant cells are able to monoubiquitinylate FANCD2 at Lys561 (Garcia-Higuera et al., 2001), whereas cells from the other groups cannot. ubiquitinylation FANCD2 normally appears during S phase of the cell cycle (Taniguchi et al., 2002a) and colocalizes with BRCA1 and RAD51 in nuclear foci. Monoubiquitinylation is required for normal cell-cycle progression following cellular exposure to MMC (Taniguchi et al., 2002a). The intriguing finding that the master-regulator ATM kinase phosphorylates FANCD2 on Ser222 after IR links the FA pathway with global signaling events during the response to damage (Taniguchi et al., 2002b).

The phenotype of FA cells includes increased chromosomal breakage/exchange, apoptosis, and reactive oxygen species (ROS), as well as prolongation of the G2 phase (for reviews see (Joenje and Patel, 2001; Bogliolo et al., 2002; D'Andrea and Grompe, 2003)). One possible mechanism is that elevated ROS leads to genotoxic stress. Many studies have suggested defects in oxygen metabolism in FA cells (reviewed by (Pagano and Youssoufian, 2003)), and at least the FANCC protein appears to have important roles in redox metabolism (Kruyt et al., 1998; Cumming et al., 2001).

Historically, FA has often been viewed as a DNA repair deficiency disorder, largely because FA cells are consistently hypersensitive to DNA cross-linking agents and have increased chromosome fragility (Sasaki and Tonomura, 1973; Auerbach and Wolman, 1976). The evidence for defects in DNA repair has been inconsistent and contradictory (Poll et al., 1984). The lack of homology between FA proteins and DNA repair proteins in lower organisms argues against the involvement of FA proteins in the enzymology of DNA repair.

Previously we cloned the human *XRCC9* gene by phenotypic correction of the MMC sensitivity of a CHO mutant (UV40) (Liu et al., 1997). Despite the UV sensitivity of UV40, *XRCC9* proved to be identical to *FANCG* cloned from FA-G lymphoblasts (de Winter et al., 1998). This convergence was unexpected because UV sensitivity is generally not associated with FA cells. In order to have an isogenic CHO *fancg* system, we produced a knockout event by gene targeting. Our studies of this new mutant support a model in which FancG, and other FA proteins, act by preventing the collapse of DNA replication forks when blocking lesions are encountered.

Results

Fancg Knockout Cells Occur at Low Frequency

Although CHO AA8 cells are hemizygous at the *FancG* locus (unpublished results), gene targeting occurs infrequently relative to random integration, requiring a screening assay to detect a knockout event in pools of transformant clones. We designed a targeting vector that contains a promoterless *neo* gene fused in-frame with *FancG* exon 3 for positive selection in G418 and the *HSV-tk* gene for negative selection in FIAU (Supplementary Figure 1A). Gene targeting through HR replaces *FancG* exons 4-6 with *neo*, reducing the genomic sequence by 1.4 kb.

Transformants were screened by PCR in pools of ~100-200 clones in three steps. First, we tested for HR of the left arm of the targeting vector by PCR amplification from *neo* to upstream *FancG* sequence (Supplementary Figure 1B). Second, pools were tested by PCR across the right arm from *neo* to downstream *FancG* sequence, and finally across the entire targeted (shortened) gene (Supplementary Figure 1C). A single pool of clones containing a knockout event was processed through two successive rounds of PCR screening, first in sub-pools of 20 clones (not shown) and then as single clones (Supplementary Figure 1D). Three targeted subclones (KO40, KO50 and KO90) (likely siblings) were isolated from > 12,000 clones, giving a targeting frequency of ~ 10^{-4}. Clone KO40, used in most future work, was confirmed by western blot to be a null mutant (Supplementary Figure 1E); we refer to these cells as *fancg* cells. Clone KO40 was complemented with CHO *FancG* BAC-clone DNA to produce a pool of six independent transformants (40BP6) that was resistant to MMC and expressed FancG at the same level as in AA8 cells (results not shown). KO40 cells have a slightly longer doubling time compared to AA8 (KO40 = 13.9 ± 0.6 hr [SEM]; AA8 = 13.0 ± 0.6 hr; and 40BP6 = 13. 7 ± 1.0 hr) and demonstrate nearly normal plating efficiency (84% versus 90% for AA8 and 40BP6).

Fancg Cells Exhibit Diverse Mutagen Sensitivity

KO40 cells exhibited increased sensitivity to a variety of agents (Figure 1; see numerical summary in legend). As expected, KO40 cells are sensitive by 2- to 7-fold to the DNA interstrand cross-linking agents diepoxybutane, mitomycin C, chloroethylnitrosourea, and chlorambucil. However, the mutant's sensitivity to the closely related compounds ethylnitrosourea (monofunctional, noncrosslinker) and chloroethylnitrosourea (bifunctional crosslinker) was similar, illustrating that KO40 cells are not preferentially sensitive to crosslinking agents. Importantly, KO40 cells have a similar degree (4-fold) of sensitivity to both methyl methanesulfonate (MMS) and methylnitrosourea (MNU) as compared with the cross-linking agents. MMS and MNU preferentially methylate DNA on nitrogen and oxygen atoms, respectively. Surprisingly, 6-thioguanine (S^6G) sensitivity increased five-fold. KO40 cells are mildly sensitive to UV-C radiation (1.5-fold), but only slightly sensitive to γ-irradiation (1.2-fold), camptothecin, and hydroxyurea. We ruled out the possibility that the S^6G sensitivity might be due to more efficient utilization by KO40 versus AA8 cells by using conditions that required the cells to grow on exogenous guanine (data not shown).

Fancg Cells Exhibit Wild-type Levels of Binding and Removal of DNA Methyl Groups

The sensitivity of KO40 cells could result from either elevated DNA damage or a defective response in removing, or coping with, base damage. We tested whether KO40 cells had increased levels of DNA damage, as reflected by single-strand breaks. No difference in spontaneous DNA damage was seen using the "comet" assay (Figure 2A). Furthermore, no difference was seen between KO40 and AA8 cells in the level of DNA breaks immediately after

an 8-min exposure to MMS (Figure 2A). In this instance, breaks arise as repair intermediates during base excision repair. These results were confirmed using N-[^{3}H] methyl-N-nitrosourea ([^{3}H]MNU) and measuring specific activity in DNA (Figure 2B). KO40 cells experience the same amount of DNA methylation as AA8 cells. Moreover, the rates of reduction in specific activity of the DNA during 24 hr post-treatment incubation were the same (Figure 2C). We conclude that *fancg* cells have normal removal of methylation damage and that their sensitivity is likely caused by defective replication, resulting in excess double-strand breaks (DSBs).

We also tested the hypothesis that the sensitivity of FA cells to MMC is caused by the increased production of reactive oxygen species (ROS) at ambient oxygen levels (Clarke et al., 1997). We measured the MMC sensitivity of cells treated for 1 hr under hypoxic conditions with 95% N_2/5% CO_2 (O_2 level < 100 ppm) (Biedermann et al., 1991). Hypoxic conditions potentiated the MMC toxicity in both cell lines, and actually increased the relative MMC sensitivity of *fancg* cells (Figure 2D).

Spontaneous Mutagenesis Is Not Elevated in *Fancg* Cells

Although spontaneous mutant frequencies are either normal or elevated in FA cells (Papadopoulo et al., 1990a; Sala-Trepat et al., 1993; Laquerbe et al., 1999), mutation rates have not been reported. Therefore, we calculated mutation rates by fluctuation analysis (Luria and Delbrück, 1943) using two statistical methods. The *aprt* locus in AA8 cells is heterozygous due to a point mutation (Thompson et al., 1980; Simon et al., 1983). *Aprt* has a higher mutation rate than *hprt* because of a high rate of deletion (Belouchi and Bradley, 1991). The spontaneous *aprt* mutation rate was not significantly different among our three cell lines (Table 1). However, at

the *hprt* locus the rate was actually reduced in KO40 cells compared to controls. This analysis was based on the surviving colonies in a high concentration of S^6G (2 µg/ml). Although this dose far exceeds those at which cell survival curves were measured, there is the possibility that the increased sensitivity of the KO40 cells to S^6G could reduce the efficiency of recovery of mutant colonies. To test this possibility, S^6G-resistance mutant frequencies of KO40 cells were compared at 2 µg/ml and 0.4 µg/ml (the equal-toxic dose compared to AA8 cells selected at 2 µg/ml). Little difference in mutant frequency (2.2×10^{-5} vs. 2.7×10^{-5}, respectively) was seen, indicating that the recovery of *hprt* mutants for KO40 was not biased by their S^6G sensitivity.

Fancg **Cells Have Elevated Rates of Gene Amplification**

Gene amplification is a manifestation of genomic instability in which megabase regions of DNA undergo increases in copy number. The process of amplification has been extensively studied at the *dhfr* locus (methotrexate resistance) and *CAD* locus (N-phosphonacetyl-L-aspartate (PALA) resistance). We find that rates of gene amplification are substantially increased (3- to 4-fold) at both loci in *fancg* cells (Table 2). 40BP6, the *FancG*-complemented mutant, had values very similar to those of the parental AA8 cells, indicating that this instability phenotype is specifically associated with the absence of FancG protein. It was shown previously that all PALA-resistant AA8 clones selected at 360 µM have amplification at the *CAD* locus (Mondello et al., 2001b). Genomic DNA from pools of 10 independent PALA-resistant clones was found to have an increase in the relative number of *CAD* gene copies with respect to another genetic marker (*APE1* locus) when compared to the DNA from cells in the respective stock cultures. In AA8 cells, the fold increase was 2.3 ± 0.8 (SEM), and in KO40 cells the fold increase was 2.8 ± 0.3,

thereby verifying amplification at the *CAD* locus and showing that the two cell lines seem to amplify to a similar extent.

Fancg Cells Have an Elevated Rate of Conversion to MMC Resistance

MMC-resistant cells are present in *fancg* cultures. Under selection at 150 nM MMC, colonies arise at high frequency (~10^{-4}). Several of these phenotypic revertant clones were isolated and examined for the level of MMC and S^6G resistance. As shown in Figure 2E for a clone designated KO40R, only MMC resistance is increased relative to KO40. KO40R cells have the same S^6G sensitivity as KO40 (see comparison indicated by right arrows in Figure 2E). KO40R cells are as resistant to MMC as the AA8 parental cells (left arrows in Figure 2E). These results suggest that some function affecting MMC metabolism is altered in these phenotypic revertants. In contrast, the parental AA8 cells do not show such phenotypic instability.

Fancg Cells with Damaged DNA are Not Delayed during S Phase

Centrifugal elutriation was used to obtain highly synchronous cell fractions of exponentially growing cultures for studies on cell cycle progression. The starting fractions were collected as predominantly late G1 cells (~10% cells in S phase incorporating BrdUrd). The tight synchrony of both AA8 and KO40 cells immediately after isolation is illustrated in Figure 3A. A synchronous wave of cells enters S phase and peaks at about 6 hr incubation, and then declines up to 12 hr. *Fancg* cells enter and progress through S phase slightly behind AA8 cells (~ 1 hr delay), which suggests a lower rate of synthesis at the beginning of S, or alternatively might reflect different positions in G1 at t = 0. Replicate cultures treated with MMS (200 μg/ml) for 8

min, before being allowed to progress, were not delayed in progression through S phase in comparison with untreated cells. (MMS was chosen for these experiments because we showed above that the rate of methyl adduct removal was the same in *fancg* and control cells.) Analysis of cell entry and exit of the G2/M phase shows a slightly prolonged G2 phase, by about 1 hr, for *fancg* cells in the absence of MMS treatment (Figure 3B). MMS damage results in increased accumulation of G2-phase cells for both cell types (Figure 3C). The MMS induced delay appears to be slightly greater for KO40 compared to WT cells.

S Phase *Fancg* Cells Have Elevated Levels of Rad51 Nuclear Foci

Nuclear foci of Rad51 protein occur spontaneously at low frequency during S-phase and increase in number and intensity in response to certain genotoxic agents such as IR, as recently reviewed in detail (Thompson and Limoli, 2003). Rad51 focus formation is thought to reflect Rad51 nucleoprotein filaments, which form at the presynaptic stage of HR. Because the Fanconi anemia pathway is linked to HR through the BRCA1/2 proteins (D'Andrea, 2003; D'Andrea and Grompe, 2003), we examined Rad51 focus formation in asynchronous KO40 cells. KO40 exhibited both a normal level of spontaneous and γ-ray-induced Rad51 foci (Figure 4A-C). These results suggest KO40 can initiate a normal HR response following γ-radiation. This result is consistent with the nearly normal IR sensitivity of KO40 cells (Figure 1).

To examine Rad51 foci associated specifically with DNA replication, we used cells synchronized in early S-phase. We saw an average increase of 2.2-fold in spontaneous Rad51 foci in KO40 versus AA8 S-phase cells (Figure 4D). Notably, the level of Rad51 protein examined by western blotting was the same in AA8 and KO40 cells (data not shown). Since KO40 cells are sensitive to killing by MMS and MMC, they likely experience more DSBs than

AA8 cells in response to these agents. We observed an appreciable increase (1.5- to 2-fold) in foci in KO40 relative to AA8 after exposure to MMS or MMC (Figure 4E and 4F). Thus, KO40 cells may have an elevated rate of HR initiation, or, alternatively, their Rad51 foci may persist longer.

Spontaneous Chromosomal Breakage and Sister-Chromatid Exchange Are Normal in *Fancg* Cells

Since increased chromosomal breakage and exchange is a prominent feature of FA, we measured spontaneous chromosomal aberrations in KO40 cells versus the two control lines. Based on a sample size of 800-1000 cells scored by two individuals, we did not see a consistent increase in aberrations in *fancg* cells (results not shown). Although there was a slight elevation in the first scoring, this increase was not reproducible. A normal level of aberrations is consistent with the nearly normal plating efficiency of KO40 cells. Sister-chromatid exchange (SCE) is one measure of homologous recombination (requiring crossing over) and is elevated in certain genome instability disorders such as Bloom syndrome. We found that the frequency of SCE is normal in *fancg* cells: 8.4 per cell (251 exchanges in 30 cells) for AA8 and 8.3 for KO40 cells (248/30); in this respect KO40 resembles NM3 (Wilson et al., 2001). These results agree with the historical observation that FA cells generally do not show altered SCE frequencies (Sperling et al., 1975).

Discussion

The Broad Genotoxicity Profile of *Fancg* Cells Provides Insight into FANCG Function

Perhaps most important, the sensitivity of KO40 cells to crosslinking agents and excess thymidine is much lower than that of the *xrcc2* and *xrcc3* hamster cell mutants that are defective in HR (Thompson, 1998; Liu et al., 1998; Lundin et al., 2002).

The two- to four-fold sensitivity of KO40 cells to methylating and ethylating agents is noteworthy. This property is generally not seen with FA lymphoblasts. However, CHO cells lack O^6-meG methyltransferase activity, making them hypersensitive to alkylation damage (Goth-Goldstein, 1980; Barrows et al., 1987). Thus, when DNA replication encounters a high burden of O^6-meG, it will result in O^6-meG:T base pairs, which are a substrate for mismatch repair. Mismatch excision is expected to result in gaps that will persist through a futile loop of excision and resynthesis (Margison and Santibanez-Koref, 2002). In the next S phase a gap will be subject to conversion to a potentially lethal DSB in one daughter chromatid. We propose that FancG helps the replication fork get past such a gap and prevent an overt DSB from arising. We sought evidence for enhanced chromosomal breaks at the first metaphase in the 14-hr samples of the cell synchrony experiments (Figure 3). There was no difference in aberration frequency between MMS-treated AA8 (6% abnormal metaphases; 80% survival) and KO40 (5% abnormal; 20% survival). This result is consistent with the idea that the excess genotoxic damage (chromosomal breaks) arises in *fancg* cells in the second cycle.

The toxicity to KO40 from S^6G occurs at ~2% substitution, a lesion density that is orders of magnitude higher than for crosslinks. Incorporated S^6G becomes methylated to form S^6-me-S^6G, which upon replication directs the incorporation of either T or C. S^6-me-S^6G:T pairs are recognized by the mismatch repair system (Swann et al., 1996; Waters and Swann, 1997). Thus, the increased single-strand breaks and defective elongation of the nascent strand in S^6G-

containing DNA (Pan and Nelson, 1990) may result from mismatch-repair incisions. A reduced ability to coordinate DNA replication with a high rate of mismatch repair, resulting in excessive DSBs at replication forks, may explain the sensitivity of *fancg* cells to S^6G. Not surprisingly, the HR-defective *xrcc3* irs1SF cells also show high S^6G sensitivity. The DNA breakage caused by S^6G appears to be akin to the spontaneous breakage that drives amplification because both KO40 and AA8 have higher amplification in the presence of S^6G (unpublished data).

DSBs Play a Role in Gene Amplification and Mutagenesis in *Fancg* Cells

Our most novel finding is the increased rate of gene amplification in KO40 cells. This process occurs at much higher rates in tumor cells than in normal diploid cells (Tlsty et al., 1989) and occurs more readily in Tp53-defective cells, including CHO (Livingstone et al., 1992). Increased amplification occurs in cells defective in mismatch repair (Chen et al., 2001; Lin et al., 2001), and, importantly, in CHO V3 cells defective in DNA-PKcs (Mondello et al., 2001b). Treatment with IR or H_2O_2 also enhances gene amplification (Mondello et al., 2002). The likely basis for the increased amplification in KO40 cells is an excess of DSBs arising during DNA replication, as depicted in our model (Figure 5) described below.

The spectrum of spontaneous *hprt* mutations in FA cell lines and T-lymphocytes is shifted toward more, and extensive, deletions over base substitutions (Papadopoulo et al., 1990a; Papadopoulo et al., 1990b; Laquerbe et al., 1999). Moreover, chemically induced *hprt* mutations are greatly suppressed in FA cells, and very few base substitution mutations are recovered at the Na^+, K^+-ATPase locus (Papadopoulo et al., 1990b). These striking results, which are analogous

to our reduced mutation frequency at the *hprt* locus in *fancg* cells, implied that FA cells are defective in a mutagenic pathway (Papadopoulo et al., 1990a). Therefore, to explain the FA hypomutability phenotype at *hprt*, we propose that in *fancg* cells potentially mutagenic lesions encountered by DNA replication forks lead to more frequent collapse of forks, with breakage of one or both parental DNA strands (Figure 5). These unrepaired DSBs reduce the recovery of *hprt* mutants. In AA8 *aprt* $^{+/-}$ cells, almost all second-step *aprt* spontaneous mutations are deletions of the Z7 allele, which arise at an unusually high rate (Simon et al., 1983; Adair et al., 1989; Belouchi and Bradley, 1991). The fact that these deletions arise by a mechanism that differs from that of *hprt* point mutations can explain why *aprt* mutations are not reduced in our *fancg* cells. In sharp contrast to the *hprt* locus in T-lymphocytes of FA patients, mutant frequencies in erythrocytes at the glycophorin-A (*GPA*) MN locus (Langlois et al., 1986) are elevated either 8- or 30-fold for NN and N0 mutations, respectively (Sala-Trepat et al., 1993). Our model accommodates these observations. N0 (+/0) allele-loss mutations should not impair the differentiation or viability of erythrocyte precursors in which they arise. NN mutations may arise by gene conversion of the MN genotype through HR occurring when a collapsed replication fork utilizes the homologous chromosome to restore replication.

We Propose a Model in Which FA Proteins Stabilize Blocked Replication Forks

The recent findings that BRCA2 is a component of the FA "pathway" (Howlett et al., 2002) and directly interacts, and colocalizes after MMC exposure, with FANCG (Hussain et al., 2003) have added a new perspective on the complexities of FA. Moreover, FANCA directly interacts with BRCA1 (Folias et al., 2002), and FANCD2 forms BRCA1-dependent nuclear foci that co-localize with BRCA1 and Rad51 (Garcia-Higuera et al., 2001; Taniguchi et al., 2002a;

Vandenberg et al., 2003). Both BRCA1 and BRCA2 are implicated in HR (see review by (Thompson and Schild, 2002)), and siRNA knockdown experiments in FA-A and FA-D2 cells suggest that BRCA2, but not BRCA1, is epistatic with FANCA and FANCD2 (Bruun et al., 2003). These findings might suggest that all FA proteins participate directly in HR, as often proposed (Joenje and Patel, 2001; D'Andrea and Grompe, 2003). However, our results for *fancg* cells indicate no defects for end points that generally reflect HR proficiency, namely SCEs, Rad51 focus formation, spontaneous chromosomal aberrations, and survival after exposure to IR. We also conclude that the common key feature of the *fancg* cytotoxic lesion is not an interstrand crosslink.

Our discovery of increased gene amplification, and increased Rad51 focus formation in synchronized S-phase cells, strongly suggest that the *fancg* defect involves the formation of excess DSBs when DNA replicates. Since Rad51 foci are generally considered to reflect the HR presynaptic stage of Rad51 nucleoprotein filament formation, our data imply that excess HR events (e.g. step E in Figure 5), arise in S-phase *fancg* cells. These events may be driven by a combination of reduced translesion synthesis (step B) and breakdown of the chickenfoot structure (step H) followed by HR-mediated repair of the DSB (not shown). The possibility of a block in HR downstream of Rad51 focus formation, causing foci to accumulate, seems less likely since *fancg* cells show normal levels of IR-induced foci. Also, if the defect in *fancg* cells were in the HR machinery, we would expect to see greatly increased spontaneous aberrations. Consistent with our data, a study of diploid fibroblasts showed elevated spontaneous Rad51 foci for all FA complementation groups except BRCA2 (Digweed et al., 2002).

In response to DNA adduct damage (e.g. cisplatin), mammalian cells exhibit a reduction in the rate of replication fork progression that is dependent on the integrity of the HR machinery

(Henry-Mowatt et al., 2003). Evidence supporting an S phase checkpoint defect in FA cell lines in response to crosslinking psoralens deserves attention (Centurion et al., 2000; Sala-Trepat et al., 2000). In our model, replication forks at sites of blocking lesions in FA cells are unstable and collapse, which may well eliminate the checkpoint signal if it arises from blocked-fork structures (see review by (Thompson and Limoli, 2003)). The G2 delay seen in our *fancg* cells, and FA cells in general, can be accounted for by unrepaired DSBs promoting the G2 checkpoint.

In summary, our data support a model (Figure 5) in which FA proteins help stabilize replication forks blocked at sites of DNA damage to prevent fork breakage in one or both parental strands. Unrepaired chromatid breaks are a cytological hallmark of FA (German, 1990). This stabilization operates in two ways. *First*, it allows time for the recruitment of mutagenic translesion polymerases. *Second*, if translesion synthesis does not occur, stabilization allows an HR-dependent template switching mechanism such as the "chickenfoot" intermediate that arises from fork reversal (Fig. 5, step E) (Michel et al., 2001; Postow et al., 2001). We presented four major lines of evidence from *fancg* cells supporting this model: (1) Sensitivity to agents that produce polymerase-blocking lesions; (2) Increased frequencies of Rad51 foci in S phase cells; (3) increased rates of gene amplification, a phenotype shared with mutant cells defective in NHEJ DSB repair; and (4) a specific reduction in *hprt* mutations, which we attribute to unrepaired fork-associated DSBs that are lethal events. Collapsed forks in FA cells can lead to decreased (*hprt*) or increased (*GPA*) spontaneous mutation rates, depending on how the specific locus and cell type govern the recovery of the mutational events.

The universal sensitivity of FA cells to interstrand crosslink agents is explained by the fact that these lesions inherently block forks with high efficiency (Akkari et al., 2000). The protective effect of antioxidants, hypoxia, and cytochrome P450 inhibitors on chromosome damage in FA

cells likely results from reducing the level of polymerase-blocking oxidized bases, such as thymine glycol. The FA proteins are apparently not needed for restarting stalled or broken forks that arise from polymerase inhibition since KO40 cells have little or no sensitivity to hydroxyurea and aphidicolin, which produce DSBs, or excess thymidine, which produces excess Rad51 foci but not DSBs (Lundin et al., 2002). The lack of sensitivity of KO40 to H_2O_2 and paraquat is consistent with the finding that these agents do not induce *hprt* mutations, which require fork blockage in our model (Bradley and Erickson, 1981; Speit et al., 1998).

In conclusion, we propose that the A/C/E/F/G/L core complex and D2 proteins, directly or indirectly, physically stabilize the blocked fork to allow either translesion synthesis or HR. An involvement of FA proteins, along with BRCA1 (Ward and Chen, 2001), at stalled replication forks fits with the finding that the BLM helicase is associated with the FA core complex (Meetei et al., 2003b). Models for BLM helicase invoke its protecting against fork breakdown or restoring productive synthesis of blocked forks (Bachrati and Hickson, 2003). Our model provides a defined conceptual framework in which to conduct future mechanistic studies of the fascinating FA proteins.

Experimental Procedures

Cell Culture

CHO cells were grown in monolayer or suspension culture in αMEM supplemented with 10% fetal bovine serum, 100 μg/ml streptomycin and 100 U/ml penicillin. Cells were counted and analyzed on a Coulter® Multisizer II. Cell doubling time was determined on suspension cultures diluted twice weekly by averaging 20 consecutive measurements. Cells were synchronized by centrifugal elutriation in a J6-M1 Centrifuge (Beckman Coulter) at 2,800 rpm with an initial flow

rate of 19-20 ml/min and 20 fractions were collected as the flow rate was incremented by 1 ml/min.

Mutagen Sensitivity

Mutagen sensitivity was determined by colony formation in 10 cm dishes. When most colonies were clearly visible by eye, dishes were rinsed with saline, fixed with 95% ethanol and stained with Gram Crystal Violet (Becton Dickinson). Exposure to genotoxic agents was as follows: UV radiation (Thompson et al., 1980); ^{137}Cs γ-irradiation, in 15-ml polypropylene tubes kept on ice; for MMS, MNU, and MMC, 1×10^5 cells in 10 ml tube suspension cultures were exposed to 37˚C for 60 min, chilled on ice, centrifuged, resuspended in fresh medium; for hydroxyurea, paraquat, and camptothecin, cells were exposed on dishes for 24 hr; for H_2O_2, cells were rinsed and exposed in PBS for 30 min at room temperature; for S^6G and thymidine cells were treated continuously. Treatment with diepoxybutane, chlorambucil, bleomycin, streptonigrin, epoxybutane, and etoposide was continuous as described (Wilson et al., 2001). The assessment of S^6G incorporation and toxicity was done using 10% dialyzed fetal bovine serum, 10 µg/ml mycophenolic acid, 10 µg/ml guanine, and varying concentrations of S^6G.

RAD51 Immunofluorescence

Ten ml of cell suspension at 1×10^5 cell/ml was treated with 5 µM MMC or 75 µg/ml MMS for 1 hr, washed once with medium, and resuspended in 10 ml fresh medium. Cells were incubated for 4 hr and then centrifuged onto glass slides at 2000 rpm for 5 min using a Cytospin® 4

cytocentrifuge (Thermo Shandon). Cells were fixed in 2% paraformaldehyde for 15 min, permeabilized in cold 0.2% Triton X-100 for 5 min, and blocked in 1% BSA for 1 hr. The slides were incubated with anti-Rad51 antibody (clone H-92, Santa Cruz Biotechnology) at 4˚C overnight (1:1000 dilution in 1% BSA), and Alexa Fluor® 488 goat anti-rabbit secondary antibody (A-11008; Molecular Probes) at room temperature for 1 hr. Glass slides were mounted using Vectashield mounting medium with DAPI (H-1200; Vector Laboratories). Fluorescence images were captured on Quips PathVysion using an Axiophot II fluorescence microscope and Rad51 foci were counted visually.

DNA Damage and Repair

Cells were exposed to N-[^{3}H]Methyl-N-nitrosourea at 46-93 ng/ml (Amersham Pharmacia Biotech) for 30 min at 37˚C in suspension culture at 2×10^{6} cell/ml in 10 ml medium made acidic by sparging with 100% CO_2. Cells were washed twice with medium, resuspended in 10 ml fresh medium, and incubated at 37˚C to allow for repair. Genomic DNA was isolated from 2 ml volumes at the times noted using DNeasy tissue kit (Qiagen) with inclusion of an RNase A digestion step.

Alkaline single-cell gel electrophoresis was used to measure DNA damage (Singh et al., 1988). Briefly, slides with cells in agarose were prepared, placed in lysis buffer composed of 1% Triton X-100, 10% DMSO, 89% stock lysing solution [2.8 M NaCl, 0.1 M Na_2EDTA, 0.01 M Trizma Base] overnight at 4˚C; after rinsing in 0.4 M Tris, pH 7.5 and immersing in 300 mM NaOH, 1 mM EDTA, pH >13.0 for 60 min, they were electrophoresed at 28 V at 300 mamps for 25 min. Slides were stained with ethidium bromide (2 µg/ml) and images of 100 cells analyzed

to determine comet distributed moment (Kent et al., 1995) using Komet4.0©: Image Analysis and Data Capture (Kinetic Imaging, Ltd., Merseyside, England).

Mutation and Gene Amplification Rates

Mutation rate was determined by fluctuation analysis (Luria and Delbrück, 1943). Replica cultures were seeded with 100 cells and grown in suspension to 1-2 × 10^6 cell/replica. For selection of *hprt* mutants, cells of each replica were plated onto 10 cm dishes at 6 × 10^5 cell/plate in 2 µg/ml S^6G. For selection of *aprt* mutants, cells were similarly plated in 80 µg/ml 8-azaadenine. Dishes were incubated for 10 days and processed as described above. Mutation rate was calculated by both Poisson Po term (Luria and Delbrück, 1943) and method of the mean (Capizzi and Jameson, 1973). Gene amplification was measured the same way as mutation rate. For selection of cells with amplified dihydrofolate reductase (*dhfr*), cells were plated, as for S^6G, in 300 nM methotrexate (MTX) or in 360 µM N-(phosphonacetyl)-L-aspartate (PALA) and 1 µM dipyridimole for selection of amplified *CAD* (carbamyl-P-synthetase, aspartate transcarbamylase, dihydro-orotase) locus. Dishes were incubated 10 days for colony formation. Verification of *CAD* gene amplification was done using real-time, quantitative PCR analysis. Equal numbers of cells from 10 PALA resistant colonies, picked in KO40 and AA8 fluctuation tests, were pooled and genomic DNA isolated. The comparative threshold cycle (C_T) method was used to quantify relative gene copy number between the *CAD* loci in DNA of PALA resistant cell pools and in DNA isolated from AA8 and KO40 stock populations. C_T values, defined as the cycle number at which fluorescence of the fluorescent reporter dye becomes

higher than the background level, were determined for the target (*CAD*) and an internal reference (*APE1*) in each sample. The reference is essential for verifying the relative starting amount of DNA in each sample. The relative copy number of the *CAD* loci of the PALA resistant (PALA-R) clones versus the stock cells was calculated as $2^{-\Delta\Delta CT}$, where $\Delta\Delta C_T = \Delta C_T^{\text{PALA-R}} - \Delta C_T^{\text{Stock}}$ and each $\Delta C_T = C_T^{\text{CAD}} - C_T^{\text{APE1}}$. Primer sequences are available upon request. PCR reactions for both primer sets and all DNA samples were performed simultaneously and in triplicate with the DyNAmo™ SYBR® Green qPCR enzyme kit (Finnzymes). PCR and fluorescence detection were performed by the DNA Engine Opticon (MJ Research). Fluorescence analysis and sample comparison was done with Opticon MONITOR analysis software. Melting curve analysis of all reactions was monitored to verify absence of nonspecific amplification.

Cell Cycle Progression

Cells were processed with or without 200 µg/ml MMS for 8 min at 37°C and collected as synchronous populations in early S-phase by centrifugal elutriation (see above). Progression through the cell cycle was determined by analyzing cell profiles at 2-hr intervals. The cells were treated with 10 µg/ml BrdUrd for the final 20 min before sample collection and fixed with 70% EtOH and stained with FITC-conjugated anti-BrdUrd antibody (BD Biosciences) and propidium iodine. Fluorescence measurements of each sample were made on a FACscan (Becton Dickinson) and the data analyzed using Cell Quest software.

ACKNOWLEDGMENTS

We thank Mary Kovacs and Martin Brown for allowing us to perform the hypoxia experiment at Stanford University. We thank Vicki Kopf and Mark Stuckenbruck for technical assistance and

Charles Limoli for suggesting the comparison between ENU and CNU. We also thank the Drug Synthesis and Chemistry Branch, Division of Cancer Treatment, National Cancer Institute, for providing PALA. This work was performed under the auspices of the U.S. Department of Energy by the University of California, Lawrence Livermore National Laboratory under Contract No. W-7405-Eng-48. Funding for this work was provided by the DOE Low-Dose Program, NCI/NIH grant CA89405, and the North West Cancer Research Fund, UK (NWCRF-CR527).

Table 1. Mutation Rates in *fancg* and *FancG*-complemented *fancg* Cells

Locus	Cell Line	Mutation Rates	
		P_0 Method (units × 10^{-7})	Mean Method (units × 10^{-7})
hprt			
	AA8 (6) [a]	1.0 ± 0.1 [b]	7 ± 1 [b]
	KO40 (5)	< 0.4 ± 0.1	< 2 ± 0.3 [c]
	40BP6 (5)	0.8 ± 0.1	4 ± 1
aprt			
	AA8 (4)	12 ± 2	100 ± 30
	KO40 (4)	7 ± 1	70 ± 20
	40BP6 (3)	8 ± 1	30 ± 10

[a] The number in parenthesis is the number of times the experiment was performed; each experiment had 12 replicate dishes.

[b] Standard error of the mean

[c] A value of 2×10^{-7} is statistically significant ($P < 0.05$) versus the AA8 value using a two-sided t test. Since no S^6G-resistant colonies were recovered in two KO40 experiments, which is indicated by "<", this is a conservative estimate of the significance.

Table 2. Rate of Mutation to Methotrexate Resistance or PALA Resistance in *Fancg* and Control Cells [a]

Cell line	Methotrexate resistance (units, × 10^{-6})		PALA resistance (units, × 10^{-6})	
	Mean [b]	SEM	Mean [c]	SEM
AA8	9	0.2	7	3
KO40	27	2.0	31	6
40BP6	9	0.9	9	4

[a] Rates were determined by the method of the mean (Capizzi and Jameson, 1973).

[b] Each experiment was done three or four times with 20 replicate cultures.

[c] Each experiment was done twice with 20 replicates.

FIGURE LEGENDS

Figure 1. Colony formation survival curves in response to DNA damaging agents and DNA replication inhibitors. The increased sensitivity of KO40/90 cells, based on D_{37} values is in the following rank order: diepoxybutane (7×), 6-thioguanine (S^6G) (5×), methyl methanesulfonate (4×), methyl-nitrosourea (4×), mitomycin C (3×), ethyl-nitrosourea (3×), chloroethyl-nitrosourea (3×), chlorambucil (2×), bleomycin (2×), streptonigrin (2×), epoxybutane (1.9×), ethyl methanesulfonate (1.6×), UV-C radiation (1.5×), etoposide (1.6×), camptothecin (1.2×), hydroxyurea (1.2×), γ-rays (1.2×), paraquat (1.0×), thymidine (1.0×), H_2O_2 (0.8×). All agents except MMS, γ-rays, and epoxybutane were tested in two or three experiments. Error bars are standard errors. Symbols: AA8, open circles; KO40, open triangles; KO90, closed triangles; and 40BP6, open squares. Note that KO40 and KO90 are sibling subclones (γ-ray and UV-C panels).

Figure 2. Measurement of single-strand breaks and methylation adducts

(A) DNA damage measured by alkaline single-cell gel electrophoresis (comet) with and without exposure to 110 μg/ml MMS for 8 min. Values are the mean of 100 data points and error bars are standard errors.

(B) DNA damage measured as specific activity of genomic DNA from cells exposed to 46-93 ng/ml [^{3}H]MNU for 30-60 min. Values represent three experiments and error bars are standard errors. 40BP6 is a pool of six transfectants of KO40 that express the hamster *FancG* gene.

(C) Rate of repair measured as specific activity of genomic DNA as a function of time following a 30 min exposure to 93 ng/ml [^{3}H]MNU. The data were normalized to the amount of damage

detected at time 0 and corrected for dilution of signal due to cell division. The graph represents one experiment.

(D) MMC sensitivity under hypoxic conditions. KO90 and AA8 cells were incubated under standard (21% O_2) or hypoxic (< 100 ppm O_2) conditions for 1 hr at 37˚C in the presence or absence of 1.5 μM MMC. Cellular sensitivity was determined by colony formation. Results are the average of three dishes (one experiment).

(E) Phenotypic suppression of MMC sensitivity in MMC-resistant derivatives of KO40 cells. One mitomycin resistant clone (KO40R) derived from KO40 was compared with AA8 and 40BP6 cultures for sensitivity to killing by MMC and S^6G in a differential cytotoxicity assay (Hoy et al., 1984) using graded doses of each agent. (From left to right and top to bottom rows, the MMC concentrations were 0, 29, 51, 93 167 and 300 nM, and the S^6G concentrations were 0, 2.5, 5.0, 10, 20 and 40 ng/ml). Twenty thousand cells per well were seeded and exposed continuously for four days (AA8) or five days (KO40 and 40BP6). The cells were then fixed with ethanol and stained; the amount of cell growth is visualized by the intensity of staining.

Figure 3. Cell cycle progression of *fancg* and control cell lines

(A) Synchronous fractions were collected from exponentially growing cultures by separating cells in late G1 phase (> 90% purity).

(B) Synchronous cells as shown in panel A were allowed to progress through the cycle with, or without, exposure to 200 μg/ml MMS for 8 min. This treatment killed 80% of KO40 cells and 20% of AA8 cells, as measured by colony forming ability. To measure the percentage of cells that were synthesizing DNA (active S), samples were pulse-labeled with BrdUrd at the time

point shown and stained with BrdUrd-specific antibody for analysis by flow cytometry. The data points are the average of two independent experiments.

(C) The data from the experiments shown in panel B are shown for the percentage of cells in G2/M at various times. The curves were smoothed mathematically for ease of viewing. The area under each curve approximates the average length of G2/M for each cell type.

Figure 4. Rad51 foci formation following γ-irradiation, MMC, or MMS exposure

(A) Cells were exposed to 8 Gy of ^{137}Cs and incubated at 37˚C for 4 hr. Foci were counted visually under a Zeiss Axiophot upright microscope. *Left panel*: AA8 cells; *right panel*, KO40 cells. The results in panels B-F represent counts from a minimum of 100 nuclei per sample.

(B & C) Distribution of foci per cell in asynchronous unirradiated and irradiated cultures

(D) Distribution of foci in untreated S phase cells from one of two experiments.

(E & F) For chemical treatments, early S-phase cells were isolated by centrifugal elutriation and exposed to 5 μM MMC or 75 μg/ml MMS for 1 hr at 37˚C, washed, and incubated at 37˚C for 4 hr before fixation. After MMC or MMS treatment the distribution of foci in *fancg* cells is shifted toward the right (one of two experiments shown).

Figure 5. Molecular model for the function of FA proteins in maintaining chromosome integrity.

(A) A DNA replication fork encounters a blocking lesion in the leading strand (e.g. adduct, crosslink, oxidized base, AP site), triggering signals that activate FANCD2 by monoubiquitinylation and implement S phase checkpoint delay. This modification of FANCD2 is a key step in stabilizing the blocked fork and requires the presence BRCA1. For simplicity subsequent events are shown for lesions other than crosslinks.

(B) Fork stabilization enables bypass of the blocking lesion by a specialized translesion polymerase that produces a mutation.

(C) If translesion synthesis does not occur, lagging-strand DNA replication continues on the intact chromatid.

(D) Fork reversal occurs through HR-mediated branch migration and repair synthesis. The interaction between FANCG and BRCA2 provides a physical link between the HR machinery and other FA proteins.

(E) Reversal of the chickenfoot intermediate by BLM and other proteins restores the replication fork, leaving the lesion in place without mutation (unless excision repair removes the lesion while the fork is regressed).

(F) In the absence of one or more FA proteins, FANCD2 is not activated and the blocked replication fork may be incised by a nuclease in the strand containing the lesion. If the lesion is a nick or gap, a DSB appears naturally.

(G) The fork collapses, resulting in chromosomal discontinuity.

(H) The chickenfoot may become a substrate of a Holliday junction (HJ) resolvase, causing fork collapse. In FA cells, this could be an alternate route of fork collapse, if, for example, FA proteins protect the chickenfoot by blocking resolvase.

(I) NHEJ, indicated by purple arrows, between broken chromatids of the same (outcome 1), or different (outcome 2), chromosomes produces translocations that appear as quadriradial figures at metaphase; triradials can arise from rejoining of isochromatid breaks with chromatid breaks (not shown). Outcome 1, which can include gene amplification and other rearrangement, is a pro-carcinogenic event.

(J) In the absence of NHEJ, chromatid breaks appear at metaphase (outcome 3).

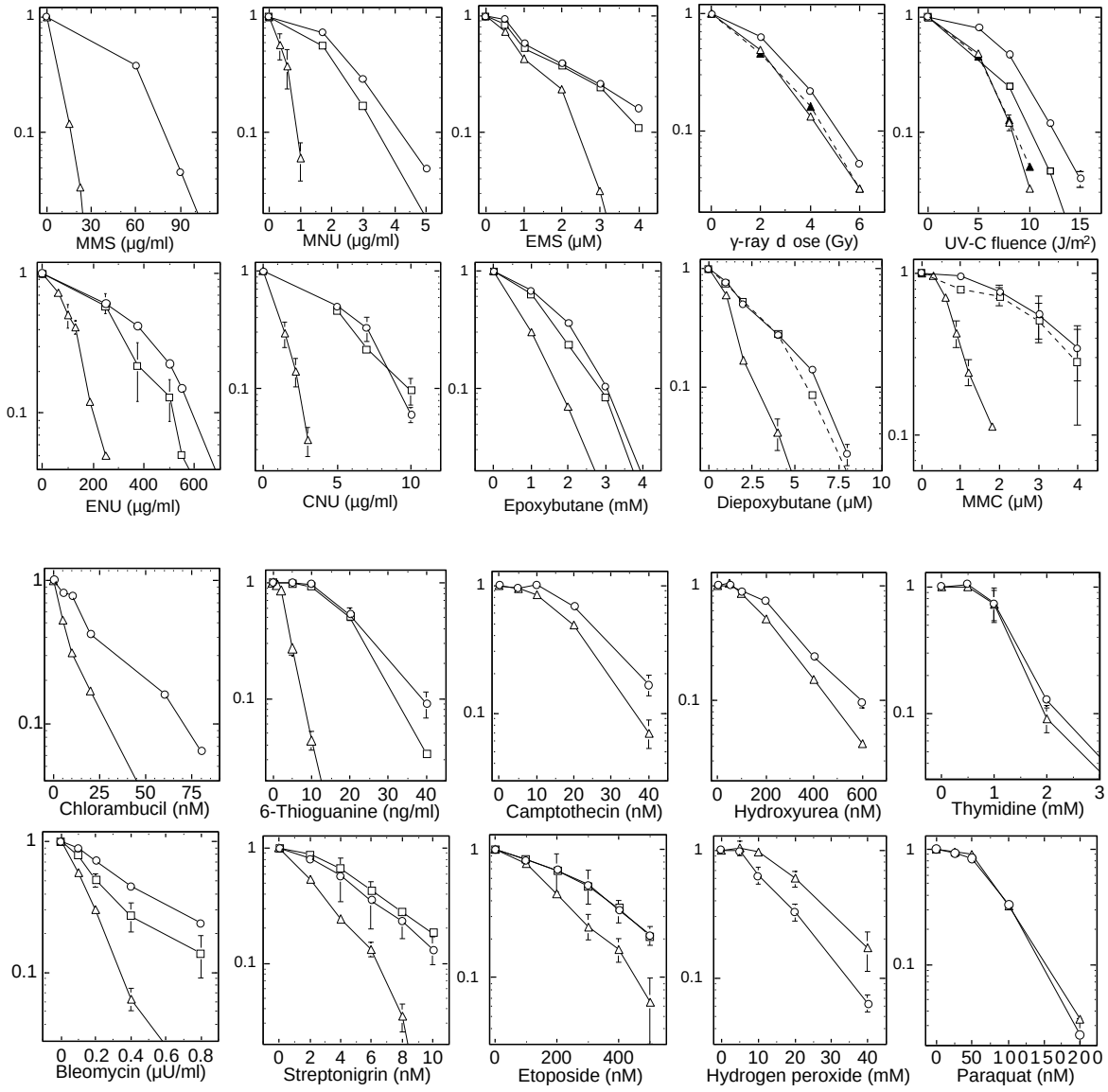
MMS (µg/ml)
MNU (µg/ml)
EMS (µM)
γ-ray d ose (Gy)
UV-C fluence (J/m²)
ENU (µg/ml)
CNU (µg/ml)
Epoxybutane (mM)
Diepoxybutane (µM)
MMC (µM)
Chlorambucil (nM)
6-Thioguanine (ng/ml)
Camptothecin (nM)
Hydroxyurea (nM)
Thymidine (mM)
Bleomycin (µU/ml)
Streptonigrin (nM)
Etoposide (nM)
Hydrogen peroxide (mM)
Paraquat (nM)

Figure 1

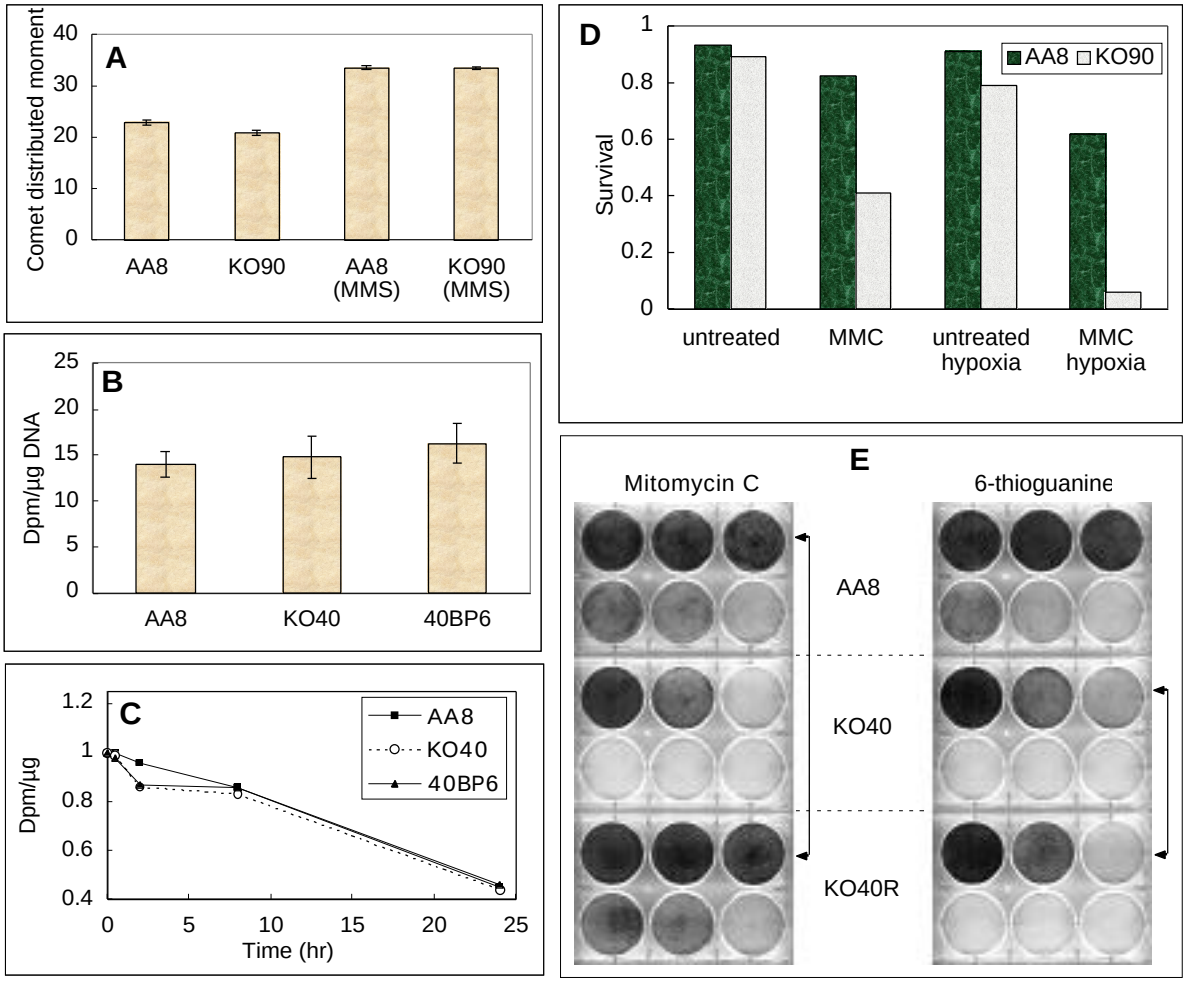
A
Comet distributed moment
40
30
20
10
0
AA8
KO90
AA8 (MMS)
KO90 (MMS)
B
Dpm/µg DNA
25
20
15
10
5
0
AA8
KO40
40BP6
C
Dpm/µg
1.2
1
0.8
0.6
0.4
0
5
10
15
20
25
Time (hr)
AA8
KO40
40BP6
D
Survival
1
0.8
0.6
0.4
0.2
0
AA8
KO90
untreated
MMC
untreated hypoxia
MMC hypoxia
E
Mitomycin C
6-thioguanine
AA8
KO40
KO40R

Figure 2

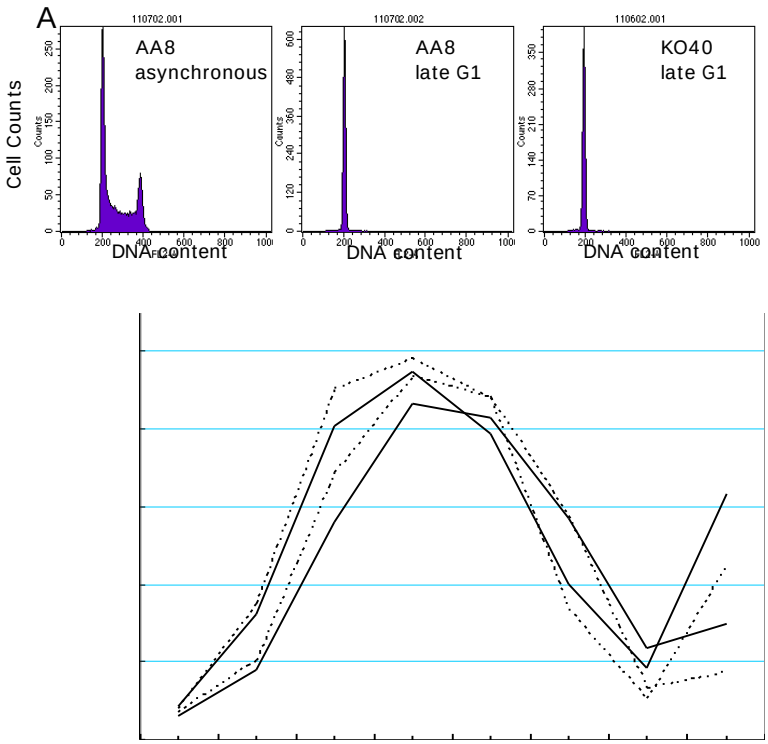
A
110702.001
AA8
asynchronous
110702.002
AA8
late G1
110602.001
KO40
late G1
Cell Counts
Counts
DNA content
DNA content
DNA content

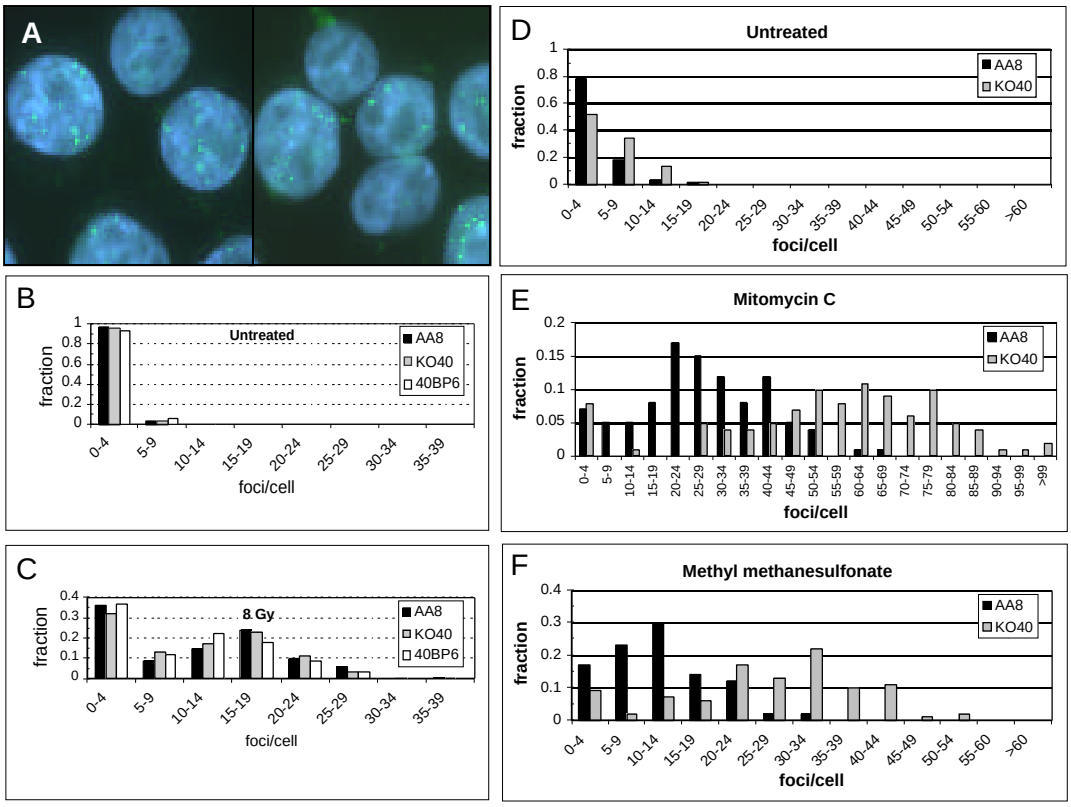
A
B
Untreated
AA8
KO40
40BP6
fraction
foci/cell
0-4
5-9
10-14
15-19
20-24
25-29
30-34
35-39
C
8 Gy
D
Untreated
40-44
45-49
50-54
55-60
>60
E
Mitomycin C
60-64
65-69
70-74
75-79
80-84
85-89
90-94
95-99
>99
F
Methyl methanesulfonate

Figure 4

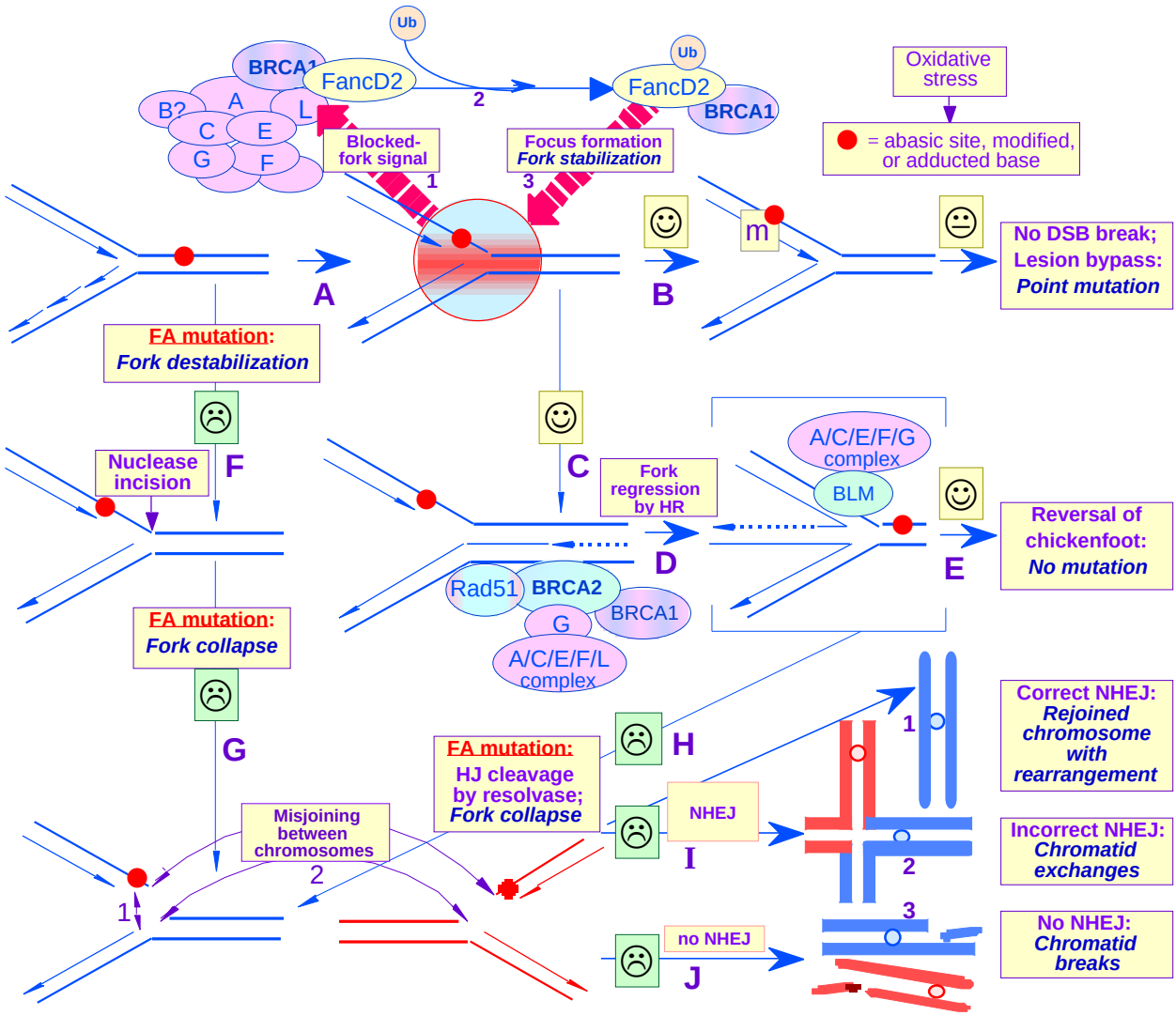
Ub
BRCA1
FancD2
B?
A
L
C
E
G
F
2
Ub
FancD2
BRCA1
Oxidative stress
= abasic site, modified, or adducted base
Blocked-fork signal
1
Focus formation
Fork stabilization
3
A
B
m
No DSB break; Lesion bypass: Point mutation
FA mutation:
Fork destabilization
Nuclease incision
F
C
Fork regression by HR
A/C/E/F/G complex
BLM
D
E
Reversal of chickenfoot: No mutation
Rad51
BRCA2
G
BRCA1
A/C/E/F/L complex
FA mutation:
Fork collapse
G
FA mutation:
HJ cleavage by resolvase;
Fork collapse
H
NHEJ
I
Misjoining between chromosomes
2
1
Correct NHEJ: Rejoined chromosome with rearrangement
Incorrect NHEJ: Chromatid exchanges
No NHEJ: Chromatid breaks
no NHEJ
J
1
2
3

Figure 5

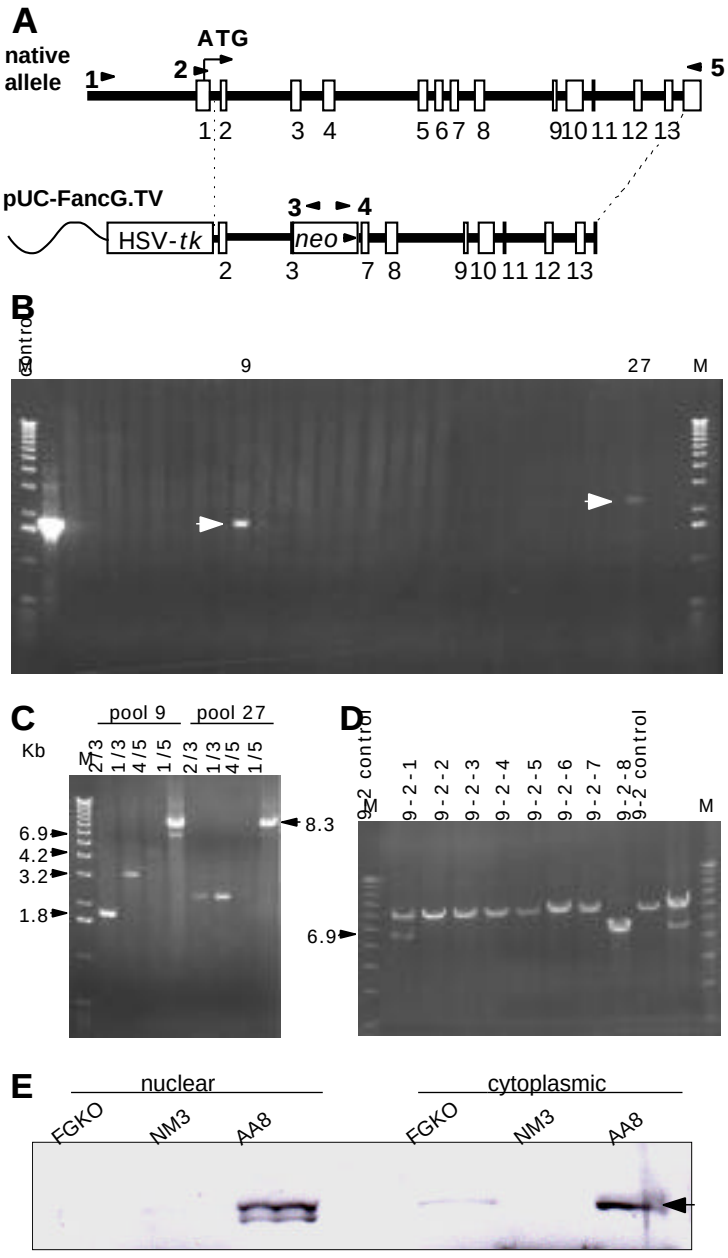

Supplementary figure S1

Legend for Supplementary Figure 1. *FancG* knockout in CHO AA8 cells.

(A), Physical map of hamster *FancG* and targeting vector pUC-FancG.TV. Open boxes represent coding regions, thick lines represent *FancG* intronic sequences, and the thin line represents plasmid sequences. HSV-*tk* and *neo* are labeled and *FancG* exons are numbered. Homologous sequences between FancG and pUC-FancG.TV are indicated by dotted lines. Arrowheads are PCR primer binding sites. Homologous recombination deletes *FancG* exons 4-6 and inserts *neo* in frame at *FancG* exon 3, allowing for PCR amplification between corresponding *FancG* and *neo* PCR primers.

(B), PCR screening pools of AA8 transformants for the presence of *FancG* knockout cells. PCR amplification was from primers 2 and 3 (targeted amplification product for PCR 2/3 is 1845 bp). Plasmid pUC-FancG.con served as a positive control. The arrowheads mark the pools containing potentially targeted cells.

(C) First round PCR positive pools 9 and 27 were examined with additional PCR primers as listed. (Targeted amplification products: PCR 1/3 = 3241 bp; PCR 4/5 = 4230 bp; and PCR 1/5 = 6860 bp. Wild-type amplification product for PCR 1/5 = 8270 bp.) The expected PCR product sizes for knockout cells are shown on the left side of the gel, and the WT PCR product size is shown on the right side.

(D), *FancG* knockout subclones were identified by PCR screening of single-cell clonal isolates using primers 1 and 5. Control sample 9-2 is a 20-cell sub-pool of pool 9, positive for gene-targeting, from which the subclones were derived. Note that subclone 9-2-7 contains no WT PCR band. Markers are 1 kb DNA ladder (Invitrogen, Carlsbad, CA).

(E) Western blot showing loss of FancG in KO40, and NM3 cells, which have a frame-shift mutation (J.E. Lamerdin, unpublished results).

Supplemental Methodology

FancG Targeting Vector Construction

Gene-targeting plasmid pUC-FancG.TV was derived from pUC19. The multiple cloning region of pUC19 was replaced with a new cloning region containing a short section of the neomycin gene (*neo*) beginning at the ATG start codon and ending at the *Eag*I restriction site by inserting an 82-mer duplex oligonucleotide between *Eco* RI and *Hind* III. The remaining *neo* sequences from *Eag*I to *Sal* I were cloned from IRES-Neo-pA (a gift from John Sedivy, Brown University) to create plasmid pUC-neo. Two *FancG* recombinant PCR fragments were amplified from a CHO *FancG* genomic BAC clone (BAC 174) and inserted into the two cloning sites of pUC-neo. The upstream *FancG* PCR fragment from intron 1 to exon 3 was 1419 bp and cloned in frame with *neo*, and the downstream *FancG* PCR fragment from exon 7 to exon 14 was 3987 bp. The thymidine kinase gene (*tk*) was isolated from pSSC-9 and blunt-end ligated into the final vector to create pUC-FancG.TV. Plasmid pUC-FancG.con was created as a positive control for gene targeting by defining PCR reactions that would identify *FancG* knockout clones. pUC-FancG.con contains an additional 655 nt 5′ of the upstream *FancG* fragment inserted into pUC-FancG.TV. PCR reactions were performed on 0.5 μg genomic DNA using High-Fidelity Platinum® Taq DNA Polymerase (Invitrogen). PCR primer sequences are available upon request.

Gene Targeting and DNA Transfection

For gene targeting, 3×10^7 cells were washed and resuspended in 1 ml cold electroporation buffer (20 mM HEPES (pH 7), 137 mM NaCl, 5 mM KCl, 0.7 mM Na_2HPO_4, 6 mM glucose), mixed with 10 μg linearized pUC-FancG.TV DNA, electroporated at 250 V/1600 μF, incubated

for 5 min on ice, and plated in T150 flasks for 24 hr to allow for *neo* expression. Cells were plated into 10-cm dishes at ~2×10^6 cell/dish in 20 ml medium containing 1.7 mg/ml G418 (Gibco Invitrogen) and incubated for 5 days at 5% CO_2 and 37˚C, after which the medium was replaced with fresh medium (supplemented with 10% dialyzed serum) containing 0.1 µM 2'-fluoro-2'-deoxy-1-beta-D-arabinofuranosyl-5-iodouracil (FIAU); cells were incubated an additional 5 days. Each dish contained a pool of ~150 drug-resistant colonies, which were harvested for freezing and DNA isolation (QIAamp® DNA Blood Mini Kit, Qiagen Inc). The frequency of G418 resistant colonies averaged 3.6×10^{-7}, and the FIAU enrichment was ~5-fold. Gene-targeted clones were identified and isolated through two rounds of screening, first into sub-pools of 20 clones and then individual clones.

References

Adair, G. M., Siciliano, M. J., Brotherman, K. A., and Nairn, R. S. Preferential loss or inactivation of chromosome Z4 *APRT* allele in CHO cells. Somat. Cell Mol. Genet. 15, 271-277. 89.

Akkari, Y.M., Bateman, R.L., Reifsteck, C.A., Olson, S.B., and Grompe, M. (2000). DNA replication is required to elicit cellular responses to psoralen-induced DNA interstrand cross-links. Mol. Cell. Biol. *20*, 8283-8289.

Auerbach, A.D. and Wolman, S.R. (1976). Susceptibility of Fanconi's anaemia fibroblasts to chromosome damage by carcinogens. Nature *261*, 494-496.

Bachrati, C.Z. and Hickson, I.D. (2003). RecQ helicases: suppressors of tumorigenesis and premature aging. Biochem. J. *374*, 577-606.

Barrows, L.R., Borchers, A.H., and Paxton, M.B. (1987). Transfectant CHO cells expressing O6-alkylguanine-DNA-alkyltransferase display increased resistance to DNA damage other than O6-guanine alkylation. Carcinogenesis *8*, 1853-1859.

Belouchi, A. and Bradley, W.E. (1991). Analysis of second-step mutations of class II and class III CHO aprt heterozygotes: chromosomal differences in deletion frequencies. Somat. Cell Mol. Genet. *17*, 277-286.

Biedermann, K.A., Wang, J., Graham, R.P., and Brown, J.M. (1991). SR 4233 cytotoxicity and metabolism in DNA repair-competent and repair-deficient cell cultures. Br. J. Cancer *63*, 358-362.

Bogliolo, M., Cabre, O., Callen, E., Castillo, V., Creus, A., Marcos, R., and Surralles, J. (2002). The Fanconi anaemia genome stability and tumour suppressor network. Mutagenesis *17*, 529-538.

Bradley, M.O. and Erickson, L.C. (1981). Comparison of the effects of hydrogen peroxide and x-ray irradiation on toxicity, mutation, and DNA damage/repair in mammalian cells (V-79). Biochim. Biophys. Acta. *654*, 135-141.

Bruun, D., Folias, A., Akkari, Y., Cox, Y. , Olson, S., and Moses, R. (2003). siRNA depletion of BRCA1, but not BRCA2, causes increased genome instability in Fanconi anemia cells. DNA Repair *2*, 1007-1013.

Capizzi, R.L. and Jameson, J.W. (1973). A table for the estimation of the spontaneous mutation rate of cells in culture. Mutat. Res. *17*, 147-148.

Centurion, S.A., Kuo, H.R., and Lambert, W.C. (2000). Damage-resistant DNA synthesis in Fanconi anemia cells treated with a DNA cross-linking agent. Exp. Cell Res. *260*, 216-221.

Chen, S., Bigner, S.H., and Modrich, P. (2001). High rate of CAD gene amplification in human cells deficient in MLH1 or MSH6. Proc. Natl. Acad. Sci. USA *98*, 13802-13807.

Clarke, A.A., Philpott, N.J., Gordon-Smith, E.C., and Rutherford, T.R. (1997). The sensitivity of Fanconi anaemia group C cells to apoptosis induced by mitomycin C is due to oxygen radical generation, not DNA crosslinking. Br. J. Haematol. *96*, 240-247.

Cumming, R.C., Lightfoot, J., Beard, K., Youssoufian, H., O'Brien, P.J., and Buchwald, M. (2001). Fanconi anemia group C protein prevents apoptosis in hematopoietic cells through redox regulation of GSTP1. Nat. Med. *7*, 814-820.

D'Andrea, A.D. (2003). The Fanconi road to cancer. Genes Dev. *17*, 1933-1936.

D'Andrea, A.D. and Grompe, M. (2003). The Fanconi anaemia/BRCA pathway. Nat. Rev. Cancer *3*, 23-34.

Davies, A.A., Masson, J.Y., McIlwraith, M.J., Stasiak, A.Z., Stasiak, A., Venkitaraman, A.R., and West, S.C. (2001). Role of BRCA2 in control of the RAD51 recombination and DNA repair protein. Mol. Cell *7*, 273-282.

de Winter, J.P., van Der Weel, L., de Groot, J., Stone, S., Waisfisz, Q., Arwert, F., Scheper, R.J., Kruyt, F.A., Hoatlin, M.E., and Joenje, H. (2000). The Fanconi anemia protein FANCF forms a nuclear complex with FANCA, FANCC and FANCG. Hum. Mol. Genet. *9*, 2665-2674.

de Winter, J.P., Waisfisz, Q., Rooimans, M.A., van Berkel, C.G., Bosnoyan-Collins, L., Alon, N., Carreau, M., Bender, O., Demuth, I., Schindler, D., Pronk, J.C., Arwert, F., Hoehn, H., Digweed, M., Buchwald, M., and Joenje, H. (1998). The Fanconi anaemia group G gene FANCG is identical with XRCC9. Nat. Genet. *20*, 281-283.

Digweed, M., Rothe, S., Demuth, I., Scholz, R., Schindler, D., Stumm, M., Grompe, M., Jordan, A., and Sperling, K. (2002). Attenuation of the formation of DNA-repair foci containing RAD51 in Fanconi anaemia. Carcinogenesis *23*, 1121-1126.

Folias, A., Matkovic, M., Bruun, D., Reid, S., Hejna, J., Grompe, M., D'Andrea, A., and Moses, R. (2002). BRCA1 interacts directly with the Fanconi anemia protein FANCA. Hum. Mol. Genet. *11*, 2591-2597.

Garcia-Higuera, I., Kuang, Y., Naf, D., Wasik, J., and D'Andrea, A.D. (1999). Fanconi anemia proteins FANCA, FANCC, and FANCG/XRCC9 interact in a functional nuclear complex. Mol. Cell. Biol. *19*, 4866-4873.

Garcia-Higuera, I., Taniguchi, T., Ganesan, S., Meyn, M.S., Timmers, C., Hejna, J., Grompe, M., and D'Andrea, A.D. (2001). Interaction of the Fanconi anemia proteins and BRCA1 in a common pathway. Mol. Cell *7*, 249-262.

German, J. (1990). The chromosome-breakage syndromes: rare disorders that provide models for studying somatic mutation. in Detection of Cancer Predisposition: Laboratory Approaches. (eds. Spatz, L., Bloom, A.D., and Paul, N.W.) March of Dimes Birth Defects Foundation, White Plains, NY, pp. 85-111

Goth-Goldstein, R. (1980). Inability of Chinese hamster ovary cells to excise O6-alkylguanine. Cancer Res. *40*, 2623-2624.

Henry-Mowatt, J., Jackson, D., Masson, J.Y., Johnson, P.A., Clements, P.M., Benson, F.E., Thompson, L.H., Takeda, S., West, S.C., and Caldecott, K.W. (2003). XRCC3 and Rad51 modulate replication fork progression on damaged vertebrate chromosomes. Mol. Cell. *11*, 1109-1117.

Howlett, N.G., Taniguchi, T., Olson, S., Cox, B., Waisfisz, Q., De Die-Smulders, C., Persky, N., Grompe, M., Joenje, H., Pals, G., Ikeda, H., Fox, E.A., and D'Andrea, A.D. (2002). Biallelic inactivation of BRCA2 in Fanconi anemia. Science *297*, 606-609.

Hoy, C.A., Salazar, E.P., and Thompson, L.H. (1984). Rapid detection of DNA-damaging agents using repair-deficient CHO cells. Mutat. Res. *130*, 321-332.

Hussain, S., Witt, E., Huber, P.A., Medhurst, A.L., Ashworth, A., and Mathew, C.G. (2003). Direct interaction of the Fanconi anaemia protein FANCG with BRCA2/FANCD1. Hum. Mol. Genet. *12*, 2503-2510.

Joenje, H. and Patel, K.J. (2001). The emerging genetic and molecular basis of Fanconi anaemia. Nat. Rev. Genet. *2*, 446-457.

Kent, C.R., Eady, J.J. , Ross, G.M., and Steel, G.G. (1995). The comet moment as a measure of DNA damage in the comet assay. Int. J. Radiat. Biol. *67*, 655-660.

Kruyt, F.A., Hoshino, T., Liu, J.M., Joseph, P., Jaiswal, A.K., and Youssoufian, H. (1998). Abnormal microsomal detoxification implicated in Fanconi anemia group C by interaction of the FAC protein with NADPH cytochrome P450 reductase. Blood *92*, 3050-3056.

Langlois, R.G., Bigbee, W.L., and Jensen, R.H. (1986). Measurements of the frequency of human erythrocytes with gene expression loss phenotypes at the glycophorin A locus. Hum. Genet. *74*, 353-362.

Laquerbe, A., Sala-Trepat, M., Vives, C., Escarceller, M., and Papadopoulo, D. (1999). Molecular spectra of HPRT deletion mutations in circulating T-lymphocytes in Fanconi anemia patients. Mutat. Res. *431*, 341-350.

Lin, C.T., Lyu, Y.L., Xiao, H., Lin, W.H., and Whang-Peng, J. (2001). Suppression of gene amplification and chromosomal DNA integration by the DNA mismatch repair system. Nucleic Acids Res. *29*, 3304-3310.

Liu, N., Lamerdin, J.E., Tebbs, R.S., Schild, D., Tucker, J.D., Shen, M.R., Brookman, K.W., Siciliano, M.J., Walter, C.A., Fan, W., Narayana, L.S., Zhou, Z.Q., Adamson, A.W.,

Sorensen, K.J., Chen, D.J., Jones, N.J., and Thompson, L.H. (1998). XRCC2 and XRCC3, new human Rad51-family members, promote chromosome stability and protect against DNA crosslinks and other damages. Mol. Cell *1*, 783-793.

Liu, N., Lamerdin, J.E., Tucker, J.D., Zhou, Z.Q., Walter, C.A., Albala, J.S., Busch, D.B., and Thompson, L.H. (1997). Cloning and characterization of the human *XRCC9* gene, which corrects chromosomal instability and mutagen sensitivity in CHO UV40 cells. Proc. Natl. Acad. Sci. USA *94*, 9232-9237.

Livingstone, L.R., White, A., Sprouse, J., Livanos, E., Jacks, T., and Tlsty, T.D. (1992). Altered cell cycle arrest and gene amplification potential accompany loss of wild-type p53. Cell *70*, 923-935.

Lo, T., Pellegrini, L., Venkitaraman, A.R., and Blundell, T.L. (2003). Sequence fingerprints in BRCA2 and RAD51: implications for DNA repair and cancer. DNA Repair *2*, 1015-1028.

Lundin, C., Erixon, K., Arnaudeau, C., Schultz, N., Jenssen, D., Meuth, M., and Helleday, T. (2002). Different roles for nonhomologous end joining and homologous recombination following replication arrest in mammalian cells. Mol. Cell. Biol. *22*, 5869-5878.

Luria, S.E. and Delbrück, M. (1943). Mutations of bacteria from virus sensitivity to virus resistance. Genetics *28*, 491-511.

Margison, G.P. and Santibanez-Koref, M.F. (2002). O6-alkylguanine-DNA alkyltransferase: role in carcinogenesis and chemotherapy. Bioessays *24*, 255-266.

Meetei, A.R., De Winter, J.P., Medhurst, A.L., Wallisch, M., Waisfisz, Q., Van De Vrugt, H.J., Oostra, A.B., Yan, Z., Ling, C., Bishop, C.E., Hoatlin, M.E., Joenje, H., and Wang, W. (2003a). A novel ubiquitin ligase is deficient in Fanconi anemia. Nat. Genet. *in press*,

Meetei, A.R., Sechi, S., Wallisch, M., Yang, D., Young, M.K., Joenje, H., Hoatlin, M.E., and Wang, W. (2003b). A multiprotein nuclearcomplex connects Fanconi anemia and Bloom syndrome. Mol. Cell. Biol. *23*, 3417-3426.

Michel, B., Flores, M.J., Viguera, E., Grompone, G., Seigneur, M., and Bidnenko, V. (2001). Rescue of arrested replication forks by homologous recombination. Proc. Natl. Acad. Sci. USA *98*, 8181-8188.

Mondello, C., Guasconi, V., Giulotto, E., and Nuzzo, F. (2002). Gamma-ray and hydrogen peroxide induction of gene amplification in hamster cells deficient in DNA double strand break repair. DNA Repair *1*, 483-493.

Mondello, C., Rebuzzini, P., Dolzan, M., Edmonson, S., Taccioli, G.E., and Giulotto, E. (2001b). Increased gene amplification in immortal rodent cells deficient for the DNA-dependent protein kinase catalytic subunit. Cancer Res. *61*, 4520-4525.

Pace, P., Johnson, M., Tan, W.M., Mosedale, G., Sng, C., Hoatlin, M., De Winter, J., Joenje, H., Gergely, F., and Patel, K.J. (2002). FANCE: the link between Fanconi anaemia complex assembly and activity. EMBO J. *21*, 3414-3423.

Pagano, G. and Youssoufian, H. (2003). Fanconi anaemia proteins: Major roles in cell protection against oxidative damage. Bioessays *25*, 589-595.

Pan, B.F. and Nelson, J.A. (1990). Characterization of the DNA damage in 6-thioguanine-treated cells. Biochem. Pharmacol. *40*, 1063-1069.

Papadopoulo, D., Guillouf, C., Mohrenweiser, H., and Moustacchi, E. (1990a). Hypomutability

in Fanconi anemia cells is associated with increased deletion frequency at the *HPRT* locus. Proc. Natl. Acad. Sci. USA *87*, 8383-8387.

Papadopoulo, D., Porfirio, B., and Moustacchi, E. (1990b). Mutagenic response of Fanconi's anemia cells from a defined complementation group after treatment with photoactivated bifunctional psoralens. Cancer Res. *50*, 3289-3294.

Poll, E.H., Arwert, F., Kortbeek, H.T., and Eriksson, A.W. (1984). Fanconi anaemia cells are not uniformly deficient in unhooking of DNA interstrand crosslinks, induced by mitomycin C or 8-methoxypsoralen plus UVA. Hum. Genet. *68*, 228-234.

Postow, L., Ullsperger, C., Keller, R.W., Bustamante, C., Vologodskii, A.V., and Cozzarelli, N.R. (2001). Positive torsional strain causes the formation of a four-way junction at replication forks. J. Biol. Chem. *276*, 2790-2796.

Sala-Trepat, M., Boyse, J., Richard, P., Papadopoulo, D., and Moustacchi, E. (1993). Frequencies of HPRT- lymphocytes and glycophorin A variants erythrocytes in Fanconi anemia patients, their parents and control donors. Mutat. Res. *289*, 115-126.

Sala-Trepat, M., Rouillard, D., Escarceller, M., Laquerbe, A., Moustacchi, E., and Papadopoulo, D. (2000). Arrest of S-phase progression is impaired in Fanconi anemia cells. Exp. Cell Res. *260*, 208-215.

Sasaki, M.S. and Tonomura, A. (1973). A high susceptibility of Fanconi's anemia to chromosome breakage by DNA cross-linking agents. Cancer Res. *33*, 1829-1836.

Siddique, M.A., Nakanishi, K., Taniguchi, T., Grompe, M., and D'Andrea, A.D. (2001). Function of the Fanconi anemia pathway in Fanconi anemia complementation group F and D1 cells. Exp. Hematol. *29*, 1448-1455.

Simon, A.E., Taylor, M.W., and Bradley, W.E.C. (1983). Mechanism of mutation at the *aprt* locus in Chinese hamster ovary cells: analysis of heterozygotes and hemizygotes. Mol. Cell. Biol. *3*, 1703-1710.

Singh, N.P., McCoy, M.T., Tice, R.R., and Schneider, E.L. (1988). A simple technique for quantitation of low levels of DNA damage in individual cells. Exp. Cell Res. *175*, 184-191.

Speit, G., Haupter, S., and Hartmann, A. (1998). Evaluation of the genotoxic properties of paraquat in V79 Chinese hamster cells. Mutat. Res. *412*, 187-193.

Sperling, K., Wegner, R.D., Riehm, H., and Obe, G. (1975). Frequency and distribution of sister-chromatid exchanges in a case of Fanconi's anemia. Humangenetik *27*, 227-230.

Swann, P.F., Waters, T.R., Moulton, D.C., Xu, Y.Z., Zheng, Q., Edwards, M., and Mace, R. (1996). Role of postreplicative DNA mismatch repair in the cytotoxic action of thioguanine. Science *273*, 1109-1111.

Taniguchi, T., Garcia-Higuera, I., Andreassen, P.R., Gregory, R.C., Grompe, M., and D'Andrea, A.D. (2002a). S-phase-specific interaction of the Fanconi anemia protein, FANCD2, with BRCA1 and RAD51. Blood *100*, 2414-2420.

Taniguchi, T., Garcia-Higuera, I., Xu, B., Andreassen, P.R., Gregory, R.C., Kim, S.T., Lane, W.S., Kastan, M.B., and D'Andrea, A.D. (2002b). Convergence of the Fanconi anemia and ataxia telangiectasia signaling pathways. Cell *109*, 459-472.

Thompson, L.H. (1998). Chinese hamster cells meet DNA repair: an entirely acceptable affair.

Bioessays *20*, 589-597.

Thompson, L.H., Fong, S., and Brookman, K. (1980). Validation of conditions for efficient detection of HPRT and APRT mutations in suspension-cultured Chinese hamster cells. Mutat. Res. *74*, 21-36.

Thompson, L.H. and Limoli, C.L. (2003). Origin, recognition, signaling, and repair of DNA double-strand breaks in mammalian cells. In Eukaryotic DNA Damage Surveillance and Repair, Ed. Keith Caldecott, Landes Press *published on-line www.landesbioscience.com*,

Thompson, L.H. and Schild, D. (2002). Recombinational DNA repair and human disease. Mutat. Res. *509*, 49-78.

Timmers, C., Taniguchi, T., Hejna, J., Reifsteck, C., Lucas, L., Bruun, D., Thayer, M., Cox, B., Olson, S., D'Andrea, A.D., Moses, R., and Grompe, M. (2001). Positional cloning of a novel Fanconi anemia gene, FANCD2. Mol. Cell *7*, 241-248.

Tischkowitz, M.D. and Hodgson, S.V. (2003). Fanconi anaemia. J. Med. Genet. *40*, 1-10.

Tlsty, T.D., Margolin, B.H., and Lum, K. (1989). Differences in the rates of gene amplification in nontumorigenic and tumorigenic cell lines as measured by Luria-Delbruck fluctuation analysis. Proc. Natl. Acad. Sci. USA *86*, 9441-9445.

Vandenberg, C.J., Gergely, F., Ong, C.Y., Pace, P., Mallery, D.L., Hiom, K., and Patel, K.J. (2003). BRCA1-independent ubiquitination of FANCD2. Mol. Cell *12*, 247-254.

Waisfisz, Q., de Winter, J.P., Kruyt, F.A., de Groot, J., van der Weel, L., Dijkmans, L.M., Zhi, Y., Arwert, F., Scheper, R.J., Youssoufian, H., Hoatlin, M.E., and Joenje, H. (1999). A physical complex of the Fanconi anemia proteins FANCG/XRCC9 and FANCA. Proc. Natl. Acad. Sci. USA *96*, 10320-10325.

Ward, I.M. and Chen, J. (2001). Histone H2AX is phosphorylated in an ATR-dependent manner in response to replicational stress. J. Biol. Chem. *276*, 47759-47762.

Waters, T.R. and Swann, P.F. (1997). Cytotoxic mechanism of 6-thioguanine: hMutSalpha, the human mismatch binding heterodimer, binds to DNA containing S6-methylthioguanine. Biochemistry *36*, 2501-2506.

Wilson, J.B., Johnson, M.A., Stuckert, A.P., Trueman, K.L., May, S., Bryant, P.E., Meyn, R.E., D'Andrea, A.D., and Jones, N.J. (2001). The Chinese hamster FANCG/XRCC9 mutant NM3 fails to express the monoubiquitinated form of the FANCD2 protein, is hypersensitive to a range of DNA damaging agents and exhibits a normal level of spontaneous sister chromatid exchange. Carcinogenesis *22*, 1939-1946.